Mechanics of Materials 165 (2022) 104179

Contents lists available at ScienceDirect

Mechanics of Materials

journal homepage: www.elsevier.com/locate/mechmat

A phenomenological constitutive model for predicting both the moderate and large deformation behavior of elastomeric materials

Stephen Kirwa Melly [a], Liwu Liu [a,*], Yanju Liu [a], Jinsong Leng [b,**]

[a] Department of Astronautical Science and Mechanics, Harbin Institute of Technology (HIT), P.O. Box 301, No. 92 West Dazhi Street, Harbin, 150001, PR China

[b] Center for Composite Materials and Structures, Harbin Institute of Technology (HIT), P.O. Box 3011, No. 2 Yikuang Street, Harbin, 150080, PR China

ARTICLE INFO

Keywords:
Hyperelasticity
Strain energy density function
Phenomenological model

ABSTRACT

Constitutive models that describe nonlinear elastic mechanical behavior are indispensable in the design of engineering components fabricated of elastomeric materials. The main drawbacks of the existing models include complexities in calibrating the model to experimental data and erroneous descriptions of multi-axial response. These challenges motivate researchers to continually formulate new or improved models with better predictive capabilities. In this work, we propose a new polynomial-type phenomenological model with linear and logarithmic dependence on the first and the second invariants respectively. Model parameters were obtained by utilizing the Levenberg-Marquardt algorithm to fit the model expression to the strain energy density data calculated from the experimental data of uniaxial tension loading. The predictive performance of our proposed model in comparison to that of three popular existing models was determined by utilizing three sets of classical experimental data from the literature with varying deformation ranges. Quantities used to relate the predicted and the experimental data include the coefficient of determination, relative errors, and average relative error (for overall behavior). The computations demonstrated that the proposed model exhibits superior predictive capabilities for the entire deformation range whilst requiring minimum efforts in obtaining its parameters, thus, exhibits the desirable features of a phenomenological hyperelastic model.

1. Introduction

With numerous advantages over physical experiments, numerical simulation is the most expedient method of assessing engineering component behavior under different loading conditions for design purposes. However, the accuracy of the simulation is dependent on the material's constitutive model. Consequently, the research on the mathematical modeling of material behavior is critical in achieving the most accurate and reliable simulation results. In the aerospace and automotive industries, elastomers are indispensable engineering materials that are extensively utilized in fabricating various components. The design process of these components is challenging as elastomeric materials exhibit a complex mechanical response to loading (Francisco Lalo et al., 2019). The complexity arises from two main factors. Firstly, these materials can withstand extremely large deformations (up to 700% engineering strains) that are recoverable upon removal of the load (hence known as *hyperelastic*). The second and the most important factor is that they exhibit a stress-strain relation that is particularly nonlinear especially at large deformations (Muhr, 2005). Accordingly, the application of linear elasticity theory to describe the material behavior is unfitting since a definite Young's modulus can't be obtained. Instead, the stress expression is derived from a strain energy density function expression that is commonly denoted as W. It represents the strain energy stored in the material per unit of the reference volume to deform it to the current configuration.

The fundamental step, therefore, in the constitutive modeling of elastomeric materials is in formulating an appropriate form of W. The formulation of W expression follows two main theories namely micromechanical and phenomenological. The micromechanical approach involves the utilization of statistical mechanics to describe the macroscopic material behavior from the microstructural level. Examples of micromechanical-based models in the literature include the eight-chain (Arruda and Boyce, 1993), the extended tube (Kaliske and Heinrich, 1999), and a recent one by Xiang et al. (Xianget al., 2018). Phenomenological models involve observing the experimental behavior of the material under different conditions of homogenous deformations

* Corresponding author.
** Corresponding author.
E-mail addresses: liuliwu_006@163.com (L. Liu), lengjs@hit.edu.cn (J. Leng).

https://doi.org/10.1016/j.mechmat.2021.104179
Received 24 September 2021; Received in revised form 26 November 2021; Accepted 26 November 2021
Available online 30 November 2021
0167-6636/

Table 1
Model parameters.

Model	Experimental data		
	Treloar (8% S vulcanized rubber)	Kawabata et al. (Isoprene rubber)	Alexander (Neoprene rubber)
Mooney-Rivlin	$C_{10} = 181825.63$, $C_{01} = -7618.22$	$C_{10} = 167833.49$, $C_{01} = 1096.05$	$C_{10} = 646828.58$, $C_{01} = -76739.76$
Yeoh	$C_{10} = 164907.76$, $C_{20} = -955.64$, $C_{30} = 33.76$	$C_{10} = 193032.94$, $C_{20} = -5221.29$, $C_{30} = 240.39$	$C_{10} = 340590.58$, $C_{20} = 2620.65$, $C_{30} = 72.322$
Gent-Thomas	$C_1 = 181825.63$ $C_2 = -82974.07$	$C_1 = 167833.49$ $C_2 = 8601.89$	$C_1 = 646828.58$ $C_2 = -909914.79$
This work	$\beta_1 = 148629.25$ $\beta_2 = -517.37$ $\beta_3 = 27.54$	$\beta_1 = 160103.53$ $\beta_2 = -1540.45$ $\beta_3 = 71.40$	$\beta_1 = 304681.99$ $\beta_2 = 3009.15$ $\beta_3 = 65.08$

Table 2
Algorithm for implementing the model equations in a Python code.

Input parameters:
1. ε_{eng} #Engineering strain
2. $\beta_1, \beta_2, \beta_3, K$ #Model constants

For all the engineering strain points, calculate:
I. $\lambda = \varepsilon_{eng} + 1$ #Stretches
II. $\mathbf{F}$ according to Eq. (9) #Deformation gradient
III. $J = \det\mathbf{F}$, $\mathbf{C} = \mathbf{F}^{\mathrm{T}}\cdot\mathbf{F}$, $\mathbf{B} = \mathbf{F}\cdot\mathbf{F}^{\mathrm{T}}$ #Volume ratio, left and right Cauchy-Green tensors
IV. $\mathbf{C}^* = J^{-2/3}\mathbf{C}$, $\mathbf{B}^* = J^{-2/3}\mathbf{B}$ #Distortional left and right Cauchy-Green tensors
V. $I_1 = \mathrm{tr}\,\mathbf{C}$, $I_2 = 0.5(I_1^2 - \mathrm{tr}(\mathbf{C}^2))$ # First and the second invariants
VI. $I_1^* = J^{-2/3}I_1$, $I_2^* = J^{-4/3}I_2$# Distortional parts of the first and second invariants
VII. Cauchy stress tensor $\boldsymbol{\sigma}$, according to Eq. (11) and Eq. (13)
VIII. Von Mises stress from the components of the Cauchy stress tensor

$$\sigma_{\mathrm{mises}} = \sqrt{\frac{1}{2}((\sigma_{11}-\sigma_{22})^2 + (\sigma_{22}-\sigma_{33})^2 + (\sigma_{33}-\sigma_{11})^2 + 6((\sigma_{12})^2 + (\sigma_{23})^2 + (\sigma_{31})^2))}$$

IX. Engineering stress from the Cauchy stress

$$\sigma_{\mathrm{eng}} = \frac{\sigma_{\mathrm{true}}}{\varepsilon_{\mathrm{eng}} + 1}$$

X. Return σ_{eng}

and thereafter fitting to mathematical equations formulated based on continuum mechanics techniques and are expressed in terms of the invariants of the Cauchy-Green deformation tensor or the principal stretches. Examples of phenomenological models include the neo-Hookean (Treloar, 1975), Mooney-Rivlin (Mooney, 1940; Rivlin, 1948), Yeoh (1993), and Ogden (Ogden, 1972). In-depth discussions on hyperelastic material models can be found in the earlier review by Steinmann et al. (Paul et al., 2012) and the most recent review by Dal et al. (2021). Phenomenological models are more prominent in the literature thanks to their relative advantages including material parameters that are easily obtained by fitting the model equation to experimental data, does not require the understanding of the material's microstructure, are computationally efficient, and apply to a wide variety of materials, unlike the micromechanical models which may be material-specific. Furthermore, phenomenological models have been the basis of more advanced constitutive relations that describe the complex mechanical behavior of soft materials. For instance, Upadhyay et al. (Upadhyay et al., 2020a) extended the Mooney-Rivlin model to capture the gel concentration-dependent behavior of hydrogels. In their other recent work (Upadhyay et al., 2020b), the authors developed a viscous dissipation potential that when combined with the Mooney-Rivlin model (as in their work) or any other hyperelastic model results in a visco-hyperelastic constitutive model that can describe both the linear and nonlinear large deformation behaviors of elastomeric materials over a wide range of strain rates. The main assumptions adhered to in formulating hyperelastic models include that the material is isotropic, the response is strain-rate independent, and generally incompressible (Bischoff et al., 2001). The incompressibility assumption leads to simplified model equations without affecting the accuracy. However, the practical behavior of elastomeric materials in certain loading conditions such as hydrostatic compression involves volume changes whereby the initial volume is reduced by up to 20% (Horgan and Murphy, 2007). Importantly, incompressible models lead to numerical problems during finite element implementations since the Poisson's ratio is 0.5 resulting in infinitely large Lame's constant. Therefore, a model that will describe the practical behavior of elastomeric materials and is suitable for finite element implementation must include the compressibility term.

The practical response of elastomeric materials to loading conditions is predominantly complex, three-dimensional, and involves multi-axial deformation modes. The predictive performance of a model in such a complex response is established by checking its ability to reproduce experimental data in three modes of homogenous deformation namely uniaxial tension, equibiaxial extension, and pure shear. We consider an excellent phenomenological model as the one that can describe the experimental behavior in each of the loading modes in an accurate manner whilst requiring a single set of model constants obtained by fitting the *W* expression to strain energy density data calculated from uniaxial tension loading stress-strain data. We refer to a model that accurately reproduces the experimental behavior in all of the three modes as having achieved a complete behavior. Unlike the uniaxial tension loading data which is readily available due to the ease of experimenting, the equibiaxial tension experiment setup is complex, requires complicated specimen geometry, is time-consuming, and involves high costs. The shortcomings of existing models include the inability to achieve complete behavior, inaccuracies at large deformations, and requiring simultaneous fitting. For instance, the Biderman model (Biderman, 1958) excellently captures the uniaxial tension and pure shear loading but posts erroneous results in equibiaxial extension. The well-known neo-Hookean model (Treloar, 1975) is suitable for small deformations as it leads to severe errors at moderate and large deformations. The Mooney-Rivlin model (Mooney, 1940; Rivlin, 1948) requires the simultaneous fitting of the uniaxial and the equibiaxial loading data and is inaccurate at large deformations. Although the fitting process for phenomenological models generally does not involve any restrictions on the material parameters since the Clausius-Duhem inequality is already applied in formulating the *W* expression, physically-reasonable predicted behavior can be achieved by imposing mathematical restrictions on the parameters such as those proposed by Upadhyay et al. (Upadhyay et al., 2019).

There have been persistent research efforts to obtain *W* expression that accurately describes the experimentally observed behavior of elastomeric materials. Hitherto, the research remains active as the researchers strive to achieve a *universal* constitutive model. As put by Destrade et al. (DestradeGiuseppe Saccomandi and Sgura, 2017), a *universal* constitutive model is the one that can satisfactorily describe the mechanical response of a given elastomeric material in all the deformation modes and strain ranges. Carroll (2011) demonstrated an interesting and unconventional method of formulating the *W* expression whereby the final form of *W* is achieved through a three-step process. Whereas the model posted remarkable predictions according to the

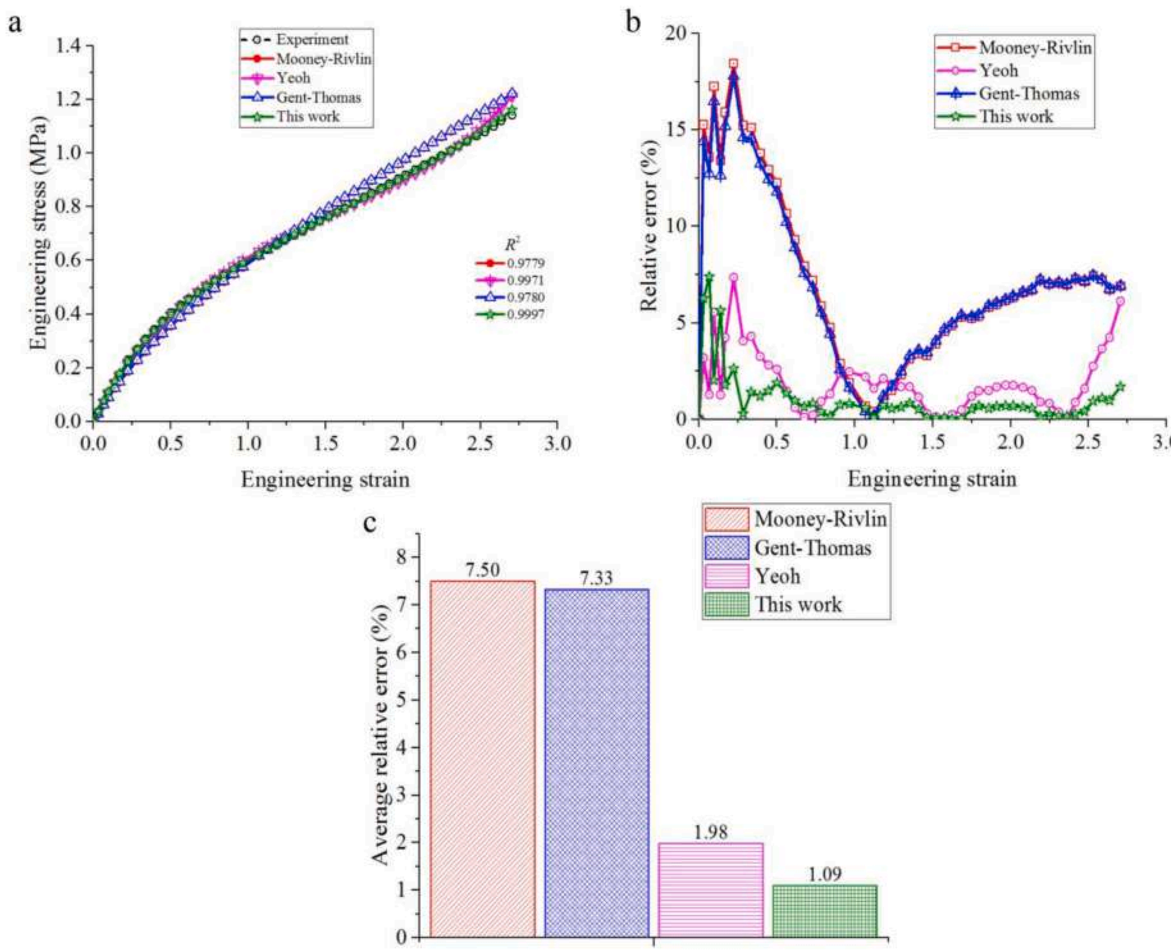

Fig. 1. Model performances in predicting the uniaxial tension loading data of Kawabata et al. (Kawabata et al., 1981). (a) stress-strain plots, (b) relative error-strain plots, and (c) the average relative error for each model.

classical experimental data by Treloar's data (Treloar, 1944); it is worth noting that the three-step process is not convenient for practical application, the incompressibility assumption makes it unsuitable for finite element implementation, the *W* expressions violates the restriction that it should have a zero value at the undeformed state and that a single fitting of the model to uniaxial extension data leads to erroneous predictions in equibiaxial tension. Melly et al. (Melly et al., 2021) addressed the drawbacks of the Carroll (2011) model by modifying the *W* expression accordingly resulting in an improved version whose parameters can be obtained in a single fitting of uniaxial data and is implementable in a finite element program. The authors (Khajehsaeid et al., 2013) proposed a micromechanical three-parameter *W* expression containing exponential-logarithmic terms of the first invariant. The idea was further pursued by Bahreman et al. (2016) where they proposed different forms of *W* expressions that combine polynomial, logarithmic, and exponential terms of the first and the second invariants. Although the authors demonstrated that their proposed *W* forms are capable of describing the behavior of elastomeric materials to a relatively higher degree of accuracy, obtaining the material parameters is quite challenging. Blaise et al. (Betchewe et al., 2020) developed a five-parameter phenomenological model that is dependent on both the first and the second invariants derived from the generalized Rivlin (Rivlin and Saunders, 1951) and Gornet et al. (2012) models respectively. Anssari-Benam and Bucchi (2021) proposed a two-parameter generalized neo-Hookean type constitutive model for elastomeric materials. The model was demonstrated to describe the experimental behavior with impressive accuracy given that it required only two parameters. However, obtaining the material parameters is a challenging task and the model is independent of the second invariant. In general, the inclusion of the second invariant in the *W* expression results in better predictions, particularly in equibiaxial loading mode. Results from a recent theoretical and experimental study carried out by Anssari-Benam et al. (Anssari-Benam et al., 2021) substantiated that the inclusion of the second invariant in formulating the *W* expression is a necessary step for more accurate model predictions.

The limitations of the existing models and the indispensability of constitutive models in the modern engineering component design inspire researchers to formulate better-performing models. The research focus is on obtaining models with desirable features such as the ability to accurately describe the experimental behavior in all the loading modes, requiring few material parameters which are obtained by fitting only the uniaxial extension data in a single fitting, applicability to the entire strain range, and implementable in a finite element program. This work proposes a phenomenological model with the mentioned features. The model is inspired by the generalized Rivlin model (Rivlin and Saunders, 1951) and requires three material parameters. To demonstrate the model's predictive capabilities, three sets of experimental data from the literature including the classical data by Treloar (1944) (8% Sulfur vulcanized rubber), Kawabata et al. (1981) (isoprene rubber), and Alexander (1968) (Neoprene rubber) are utilized. The data in this work represents both the moderate (Kawabata et al.) and large (Treloar and Alexander) deformations. Using the coefficient of determination and the relative error to quantify the model's ability to reproduce the experimental data, it is demonstrated that it performs better than well-known hyperelastic models including Mooney-Rivlin (Mooney, 1940; Rivlin, 1948), Yeoh (1993), and the Gent-Thomas (Gent and Thomas, 1958).

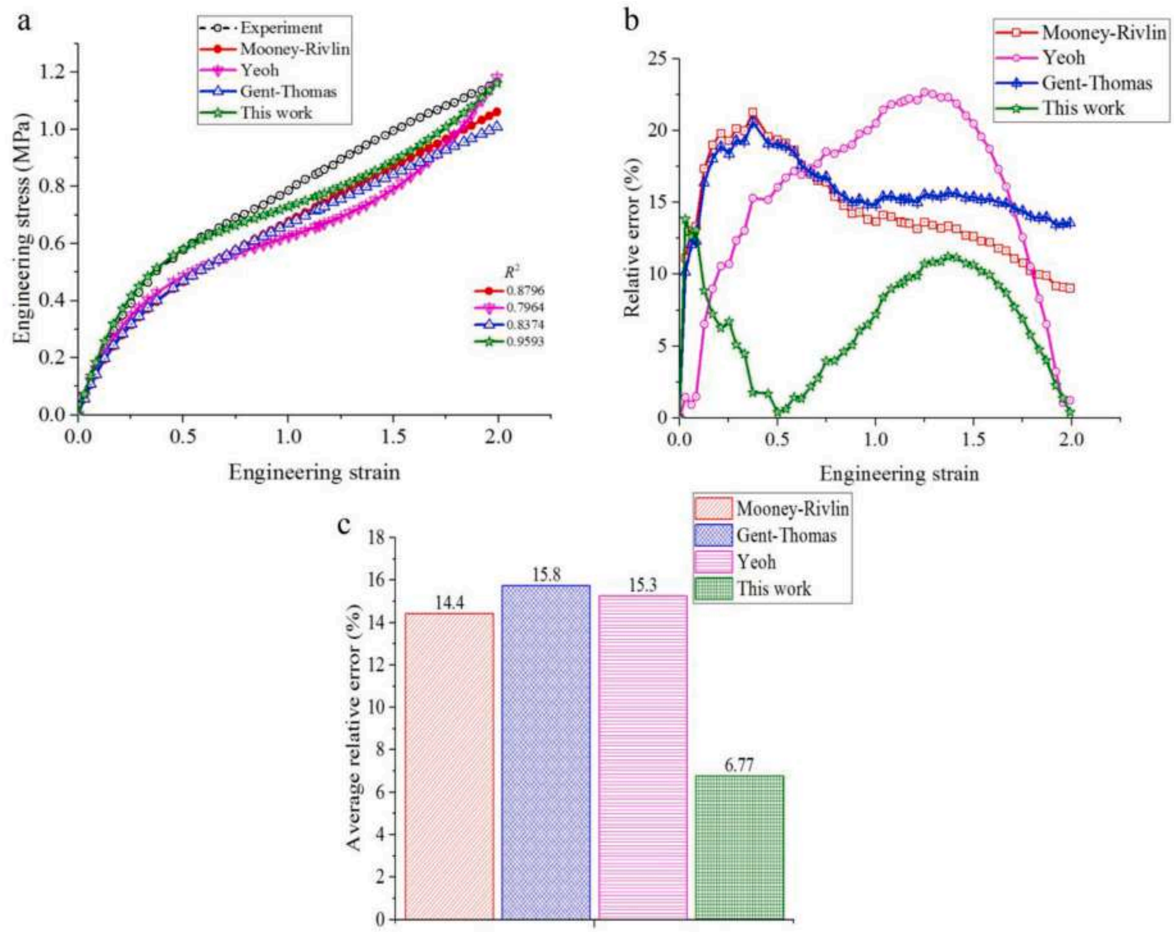

Fig. 2. Model performances in reproducing the equibiaxial loading data of Kawabata et al. (Kawabata et al., 1981). (a) predicted and the experimental stress-strain plots, (b) relative error-strain plots, and (c) the average relative error for each model.

2. Constitutive modeling

2.1. Proposed strain energy density function

The most significant development in the phenomenological theory of hyperelasticity was the model (also known as the polynomial model) proposed by Rivlin and Saunders (1951) in which W is expressed as a double-sum infinite power series of the two invariants of Cauchy-Green deformation tensor as shown in Eq. (1).

$$W = \sum_{p=0}^{N} \sum_{q=0}^{N} C_{pq} (I_1 - 3)^p (I_2 - 3)^q \tag{1}$$

The terms C_{pq} in Eq. (1) represents the model parameters and the first parameter C_{00}, is taken to be zero so that W vanishes at the undeformed state, I_1 and I_2 are the first and the second invariants of Cauchy-Green deformation tensor respectively given by Eq. (2).

$$\begin{aligned} I_1 &= \mathrm{tr}\ \mathbf{C} \\ I_2 &= \frac{1}{2}\left[(I_1)^2 - tr\left(\mathbf{C}^2\right)\right] \end{aligned} \tag{2}$$

where $\mathbf{C}$ is the right Cauchy-Green deformation tensor given by $\mathbf{C} = \mathbf{F}^{\mathrm{T}} \cdot \mathbf{F}$ and $\mathbf{F}$ is the deformation gradient. For $N = 1$, $N = 2$, and $N = 3$, the number of model parameters required are 3, 8, and 15 respectively. This is the main drawback of the polynomial model; a large number of parameters complicates the fitting process and does not necessarily improve the predictive capabilities. Moreover, the models derived from it such as the Mooney-Rivlin (Mooney, 1940; Rivlin, 1948) (obtained when the first two terms of expanded Eq. (1) are considered) require simultaneous fitting for stable parameters. To circumvent these drawbacks, we propose a new form of a polynomial model whose expression is a single-sum infinite series of the first and the second invariants. As shown in Eq. (3), the proposed model takes the logarithmic form for the second invariant term as it has been proven to be more accurate than the linear form (Dal et al., 2021). Importantly, it drastically reduces the number of required parameters. For instance, if $N = 3$, the number of parameters required is 3 in contrast to 15 for Eq. (1).

$$W = \sum_{i=1}^{N} \beta_i \left[I_1 + \ln\left(\frac{I_2}{3}\right) - 3 \right]^i \tag{3}$$

where β_i are the material parameters. The W expression presented in equation (3) is based on the common assumption of incompressibility. To model the compressible behavior of elastomeric materials, it is necessary to additively decompose the W expression into distortional and volumetric parts as shown in Eq. (4) (Murphy and Rogerson, 2018). The former represents part of W that is responsible for shape change whereas the latter for volume change.

$$W = W_{\mathrm{d}}\left(I_1^*, I_2^*\right) + W_{\mathrm{v}}(J) \tag{4}$$

where the subscripts d and v represent the distortional and the volumetric parts respectively, J is the volume ratio given by $J = \det\mathbf{F}$ whereas the distortional parts of I_1 and I_2 are given by $I_1^* = J^{-2/3} I_1$ and $I_2^* = J^{-4/3} I_2$ respectively. Whilst there are numerous forms of W_{v} in the literature (Doll and Schweizerhof, 2000), the most commonly used form (see Eq. (5) (Horgan and Murphy, 2009)) is utilized in this work.

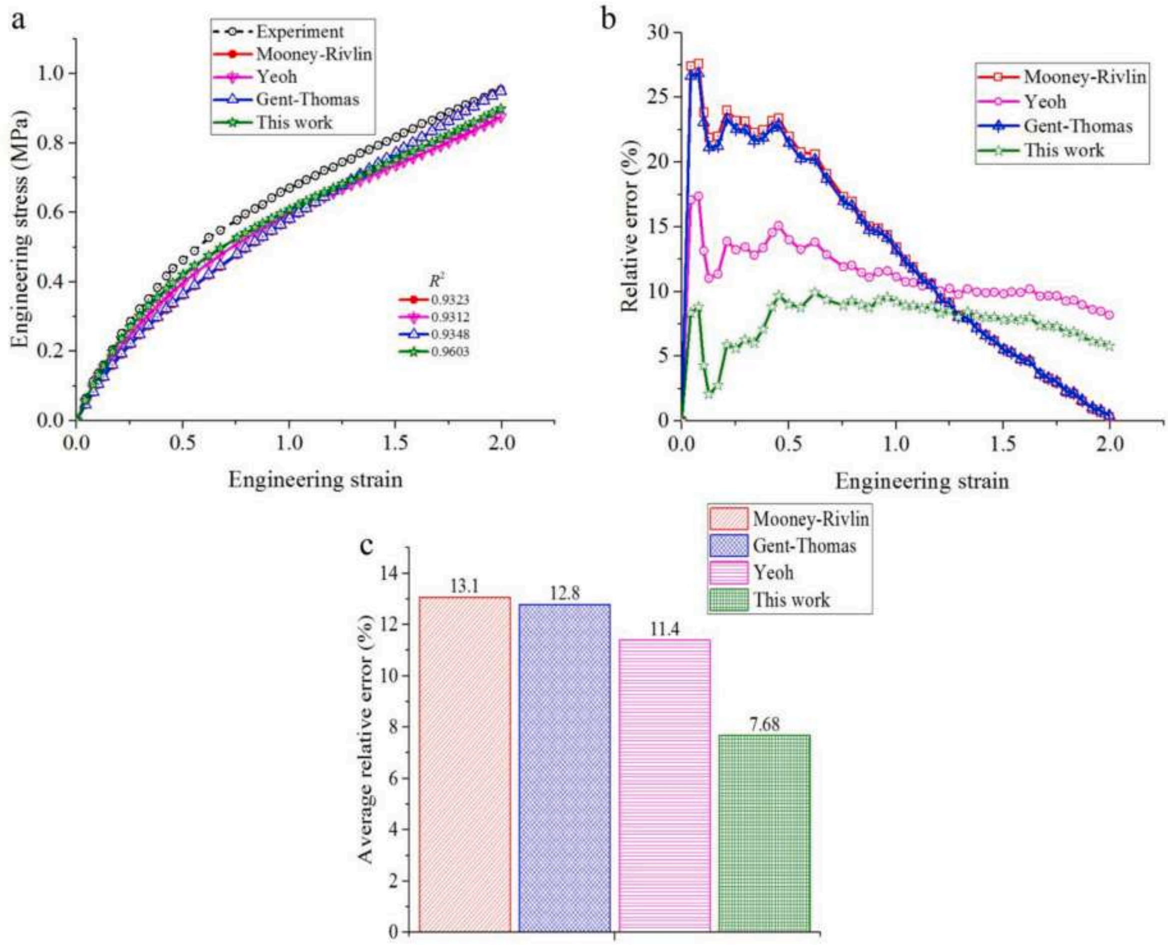

Fig. 3. Model performances in reproducing the pure shear loading data of Kawabata et al. (Kawabata et al., 1981). (a) model and experimental engineering stress-strain curves, (b) plots of relative error against strain, and (c) the average relative errors.

$$W_v = \frac{K}{2}(J-1)^2 \tag{5}$$

The constant K in Eq. (5) is the bulk modulus of the material. With Eqs. (3)–(5), we obtain the compressible version of our proposed model as shown in Eq. (6).

$$W = \sum_{i=1}^{N} \beta_i \left[I_1^* + \ln\left(\frac{I_2^*}{3}\right) - 3 \right]^i + \frac{K}{2}(J-1)^2 \tag{6}$$

The order, N, influences the accuracy of the predicted data, especially for large deformations. The capability of the model to describe the upturn of the engineering stress-strain curve at large deformations increases with increasing N to a certain value. The optimal value of N should be carefully determined to avoid complicating the model with a large number of parameters. As will be demonstrated in section 4.5, this value was found to be 3 for our model. Re-writing Eq. (6) with $N = 3$, we obtain the explicit W expression for our proposed model as shown in Eq. (7).

$$W = \beta_1 \left[I_1^* + \ln\left(\frac{I_2^*}{3}\right) - 3 \right] + \beta_2 \left[I_1^* + \ln\left(\frac{I_2^*}{3}\right) - 3 \right]^2 + \beta_3 \left[I_1^* + \ln\left(\frac{I_2^*}{3}\right) - 3 \right]^3 + \frac{K}{2}(J-1)^2 \tag{7}$$

where β_1, β_2 and β_3 are the model parameters.

2.2. Stress-strain relation

For a phenomenological model with dependence on the first two invariants and considering compressibility of the material, the derivation process of the Cauchy stress $\boldsymbol{\sigma}$ expression from the W expression was meticulously presented in the mechanics of solid polymers book by Bergström (2015). Consequently, it will just be stated in this work and readers may check on the mentioned book for a step-by-step derivation process. For arbitrary loading of a hyperelastic material and considering volume changes during deformation, the $\boldsymbol{\sigma}$ tensor expression is given in Eq. (8).

$$\boldsymbol{\sigma} = \frac{2}{J}\left(\frac{\partial W}{\partial I_1^*} + I_1^* \frac{\partial W}{\partial I_2^*}\right)\mathbf{B}^* - \frac{2}{J}\frac{\partial W}{\partial I_2^*}(\mathbf{B}^*)^2 + \left(\frac{\partial W}{\partial J} - \frac{2I_1^*}{3J}\frac{\partial W}{\partial I_1^*} - \frac{4I_2^*}{3J}\frac{\partial W}{\partial I_2^*}\right)\mathbf{I} \tag{8}$$

where $\mathbf{B} = \mathbf{F}\cdot\mathbf{F}^{\mathrm{T}}$ is the left Cauchy-Green deformation tensor whereas $\mathbf{B}^*$ is its distortional part given by $\mathbf{B}^* = J^{-2/3}\mathbf{B}$. The response in a specific loading mode is determined by its corresponding $\mathbf{F}$ expression given in Eq. (9).

$$\mathbf{F}_{ut} = \begin{bmatrix} \lambda & 0 & 0 \\ 0 & \frac{1}{\sqrt{\lambda}} & 0 \\ 0 & 0 & \frac{1}{\sqrt{\lambda}} \end{bmatrix}, \quad \mathbf{F}_{eb} = \begin{bmatrix} \lambda & 0 & 0 \\ 0 & \lambda & 0 \\ 0 & 0 & \frac{1}{\lambda^2} \end{bmatrix}, \quad \mathbf{F}_{ps} = \begin{bmatrix} \lambda & 0 & 0 \\ 0 & 1 & 0 \\ 0 & 0 & \frac{1}{\lambda} \end{bmatrix} \tag{9}$$

where the subscripts ut, eb, and ps stand for uniaxial tension, equibiaxial extension, and pure shear respectively. To get the $\boldsymbol{\sigma}$ expression for our

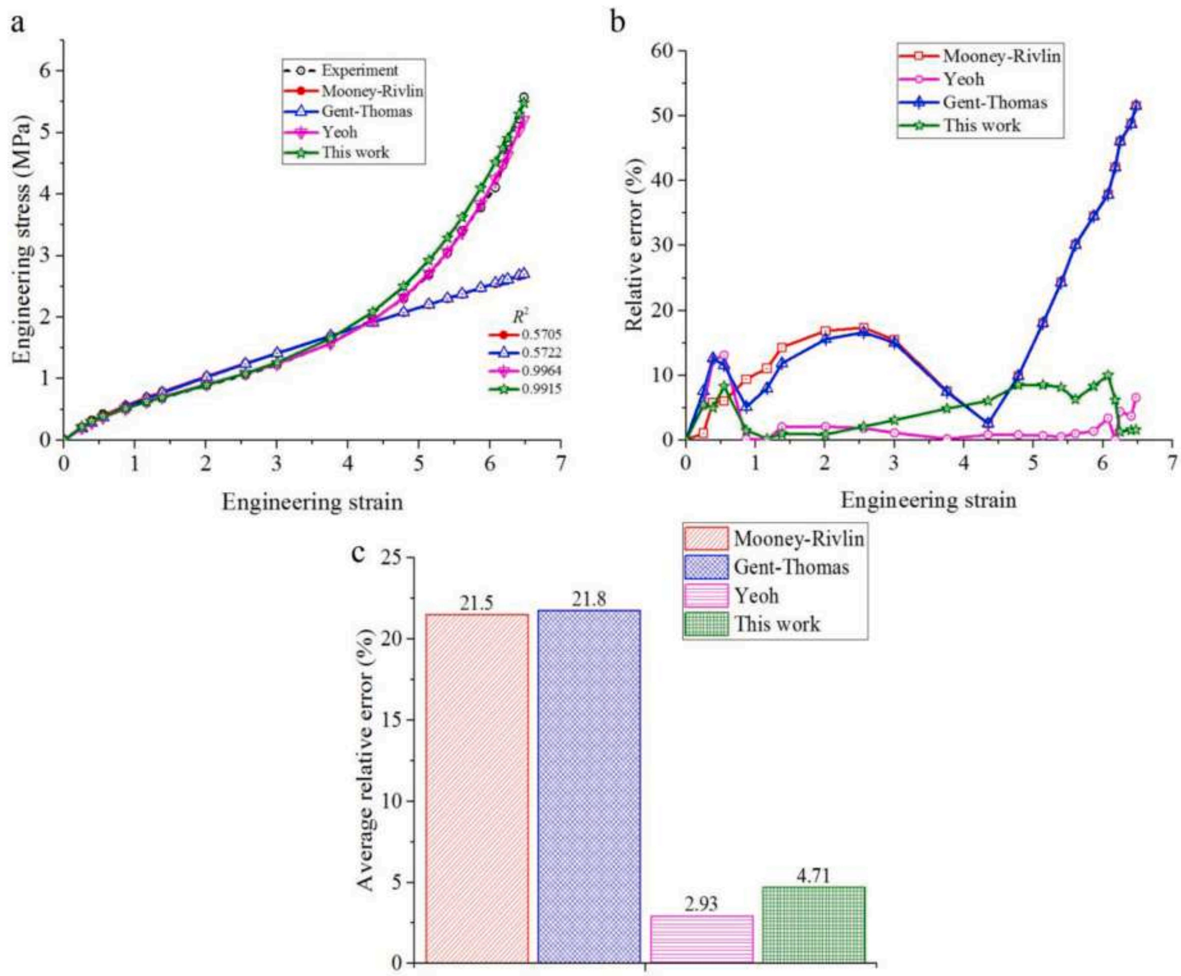

Fig. 4. Comparisons of model performances in describing the uniaxial tension behavior of vulcanized rubber by Treloar (Treloar, 1944). (a) experimental and the predicted stress-strain curves, (b) relative error-strain plots, and (c) the average relative errors.

proposed model, it is necessary to obtain the partial derivatives of its W expression given in Eq. (7) with respect to I_1^*, I_2^* and J as shown in Eq. (10).

$$
\begin{aligned}
\frac{\partial W}{\partial I_1^*} &= \beta_1 + 2\beta_2\left[I_1^* + \ln\left(\frac{I_2^*}{3}\right) - 3\right] + 3\beta_3\left[I_1^* + \ln\left(\frac{I_2^*}{3}\right) - 3\right]^2 \\
\frac{\partial W}{\partial I_2^*} &= \left(\frac{1}{I_2^*}\right)\left\{\beta_1 + 2\beta_2\left[I_1^* + \ln\left(\frac{I_2^*}{3}\right) - 3\right] + 3\beta_3\left[I_1^* + \ln\left(\frac{I_2^*}{3}\right) - 3\right]^2\right\} \\
\frac{\partial W}{\partial J} &= K(J-1)
\end{aligned} \tag{10}
$$

Substituting Eq. (10) to Eq. (8) yields the proposed model's $\boldsymbol{\sigma}$ tensor expression for arbitrary loading given in Eq. (11).

$$
\begin{aligned}
\boldsymbol{\sigma} = &\frac{2}{J}\left\{\beta_1 + 2\beta_2\left[I_1^* + \ln\left(\frac{I_2^*}{3}\right) - 3\right] + 3\beta_3\left[I_1^* + \ln\left(\frac{I_2^*}{3}\right) - 3\right]^2\left(1 + \frac{I_1^*}{I_2^*}\right)\right\}(\mathbf{B}^*) - \\
&\frac{2}{JI_2^*}\left\{\beta_1 + 2\beta_2\left[I_1^* + \ln\left(\frac{I_2^*}{3}\right) - 3\right] + 3\beta_3\left[I_1^* + \ln\left(\frac{I_2^*}{3}\right) - 3\right]^2\right\}(\mathbf{B}^*)^2 + \\
&\left\{\begin{array}{l} K(J-1) - \dfrac{2I_1^*}{3J}\left\{\beta_1 + 2\beta_2\left[I_1^* + \ln\left(\dfrac{I_2^*}{3}\right) - 3\right] + 3\beta_3\left[I_1^* + \ln\left(\dfrac{I_2^*}{3}\right) - 3\right]^2\right\} - \\ \dfrac{4}{3J}\left\{\beta_1 + 2\beta_2\left[I_1^* + \ln\left(\dfrac{I_2^*}{3}\right) - 3\right] + 3\beta_3\left[I_1^* + \ln\left(\dfrac{I_2^*}{3}\right) - 3\right]^2\right\} \end{array}\right\}\mathbf{I}
\end{aligned} \tag{11}
$$

As mentioned in the introductory part of this work, the performance of the proposed model will be compared with that of popular existing models including Mooney-Rivlin (Mooney, 1940; Rivlin, 1948), Yeoh (1993), and the Gent-Thomas (Gent and Thomas, 1958). For convenience, compressible versions of the W expressions of these models are presented in Eq. (12).

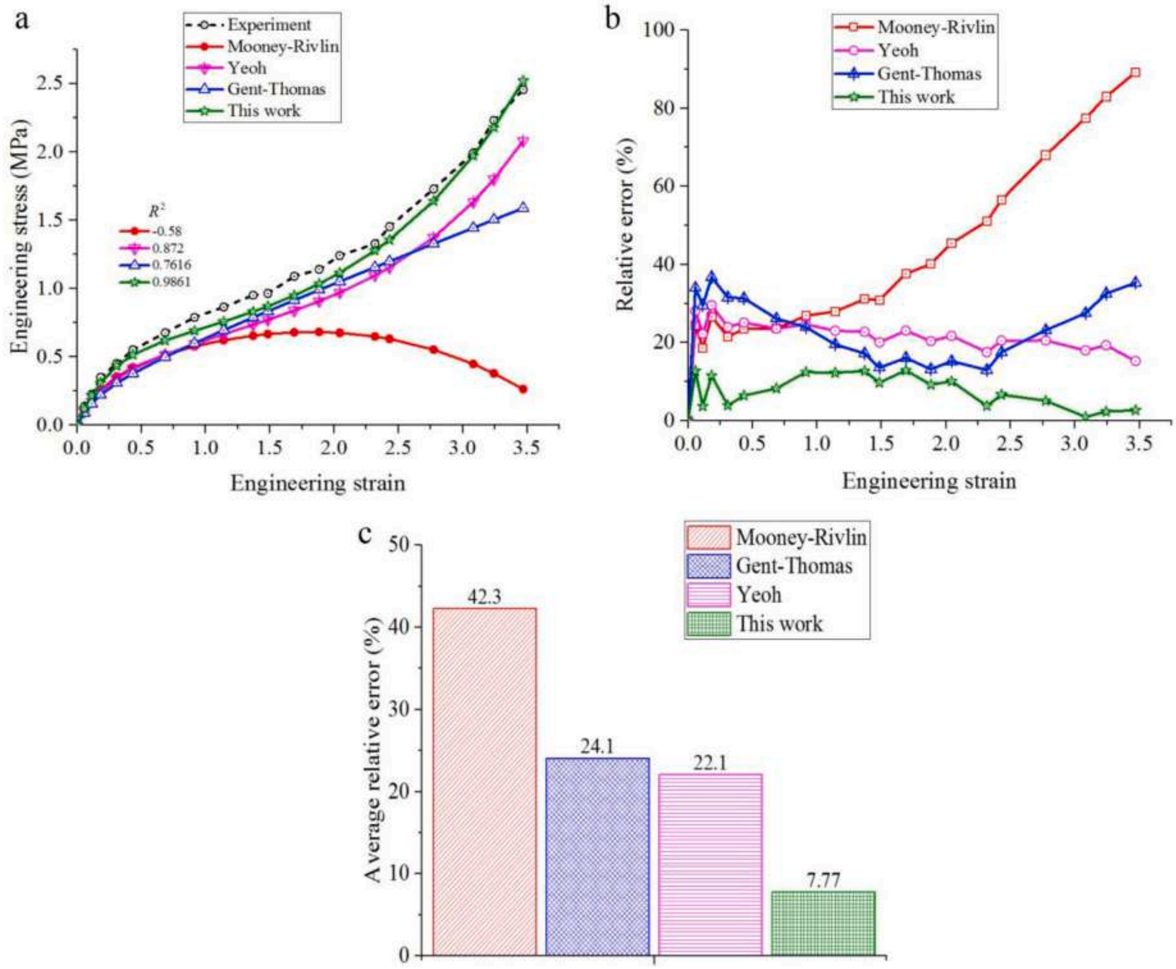

Fig. 5. Model performances in reproducing the equibiaxial tension loading data of vulcanized rubber by Treloar (Treloar, 1944). (a) model-predicted and experimental engineering stress-strain curves, (b) relative error-strain plot, and (c) the average relative errors.

$$
\begin{aligned}
W_{\mathrm{YH}} &= C_{10}\left(I_1^* - 3\right) + C_{20}\left(I_1^* - 3\right)^2 + C_{30}\left(I_1^* - 3\right)^3 + \frac{K}{2}(J-1)^2 \\
W_{\mathrm{MR}} &= C_{10}\left(I_1^* - 3\right) + C_{01}\left(I_2^* - 3\right) + \frac{K}{2}(J-1)^2 \\
W_{\mathrm{GT}} &= C_1\left(I_1^* - 3\right) + C_2 \ln\left(\frac{I_2^*}{3}\right) + \frac{K}{2}(J-1)^2
\end{aligned} \tag{12}
$$

where the subscripts $\mathrm{YH}, \mathrm{MR},$ and GT stand for Yeoh, Mooney-Rivlin, and Gent-Thomas respectively. According to Eq. (8), the corresponding $\boldsymbol{\sigma}$ expressions are given in Eq. (13).

$$
\begin{aligned}
\boldsymbol{\sigma}_{\mathrm{YH}} &= \frac{2}{J}\left[C_{10} + 2C_{20}\left(I_1^* - 3\right) + 3C_{30}\left(I_1^* - 3\right)^2\right]\mathbf{B}^* + \left[K(J-1) - \frac{2I_1^*}{3J}\left(C_{10} + 2C_{20}\left(I_1^* - 3\right) + 3C_{30}\left(I_1^* - 3\right)^2\right)\right]\mathbf{I} \\
\boldsymbol{\sigma}_{\mathrm{MR}} &= \frac{2}{J}\left(C_{10} + I_1^* C_{01}\right)\mathbf{B}^* - \frac{2}{J}C_{01}\left(\mathbf{B}^*\right)^2 + \left[K(J-1) - \frac{2I_1^*}{3J}C_{10} - \frac{4I_2^*}{3J}C_{01}\right]\mathbf{I} \\
\boldsymbol{\sigma}_{\mathrm{GT}} &= \frac{2}{J}\left(C_1 + I_1^*\frac{C_2}{I_2^*}\right)\mathbf{B}^* - \frac{2}{J}\frac{C_2}{I_2^*}\left(\mathbf{B}^*\right)^2 + \left[K(J-1) - \frac{2I_1^*}{3J}C_1 - \frac{4I_2^*}{3J}\frac{C_2}{I_2^*}\right]\mathbf{I}
\end{aligned} \tag{13}
$$

3. Model implementation

To obtain the predicted Cauchy stress data, the model $\boldsymbol{\sigma}$ expressions given in Eq. (11) and Eq. (13) are implemented in computer codes written in Python language. The model parameters required during implementation are obtained by fitting the W expressions given in Eq. (7) and Eq. (12) to strain energy density-strain data (obtained by calculating the area under uniaxial tension engineering stress-strain curves). The strain energy density and engineering strain relate in a highly nonlinear manner, particularly for large deformations. Consequently, fitting of the W expressions for model constants is a nonlinear least-squares problem. The Levenberg-Marquardt Algorithm (LMA) (Levenberg, 1944; Marquardt, 1963), which is the most widely used optimization algorithm due to its superior performance over other

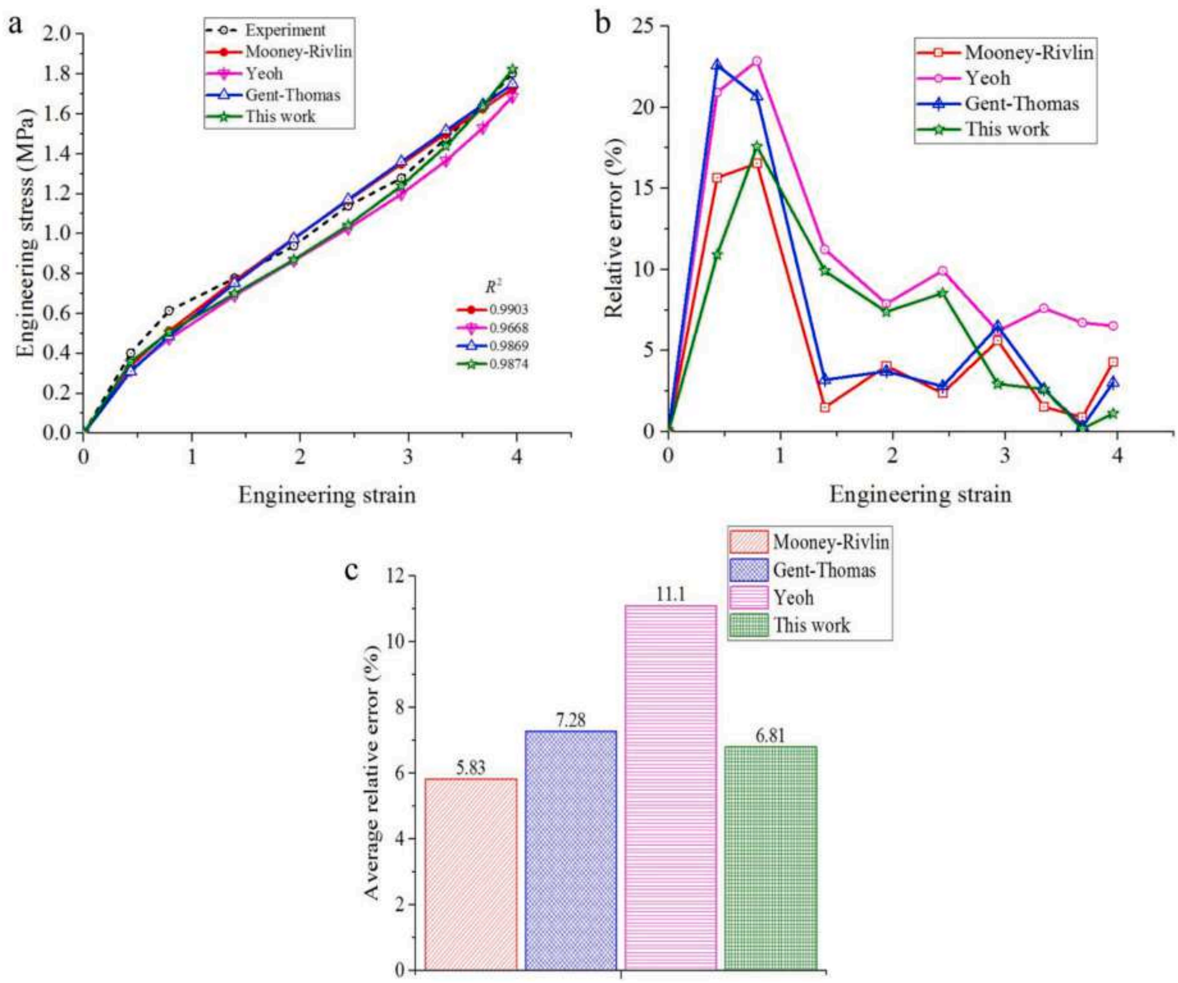

Fig. 6. Model performances in reproducing the pure shear loading data of vulcanized rubber by Treloar (Treloar, 1944). (a) model-predicted and experimental engineering stress-strain curves, (b) relative error-strain plot, and (c) the average relative errors.

methods, is utilized in this work. The flowchart for implementing the LMA in Python code is presented in our previous work (Melly et al., 2021). The model parameters obtained for each of the experimental data are given in Table 1. It is worth noting that for the bulk modulus K, a value $500MPa$ was used for all the experimental data.

Taking the proposed model whose $\boldsymbol{\sigma}$ tensor expression is given in Eq. (11) as an example, the algorithm for implementing it in Python code is shown in Table 2. It is worth noting that the $\boldsymbol{\sigma}$ tensor expression yields true stress (Cauchy stress) components whereby the scalar value (Von Mises) must be obtained and converted to engineering stress as shown in the algorithm.

4. Results and discussion

We now present the performances of our proposed model (referred to as *this work*), Mooney-Rivlin (Mooney, 1940; Rivlin, 1948), Yeoh (1993), and Gent-Thomas (Gent and Thomas, 1958) models in describing the experimental data of isoprene rubber by Kawabata et al. (1981), 8% S vulcanized rubber by Treloar (1944), and neoprene rubber by Alexander (1968). To quantify the overall accuracy of the model's predictions in each loading mode, we obtained the coefficient of determination, R^2, whose expression is given in Eq. (14).

$$R^2 = 1 - \frac{\sum_{i=1}^{n} (e_i - p_i)^2}{\sum_{i=1}^{n} (e_i - e_m)^2} \tag{14}$$

where n, e_i, p_i and e_m are the size of the data points, experimental data at point i, predicted data at point i, and the mean experimental data respectively. Generally, the R^2 values range from zero to one with the latter meaning that there is a perfect match between the predicted and the experimental data. It is not unusual to obtain negative values which would mean that the average value of the predicted data is way far from the mean value of the experimental data. To visualize the predictive performance of the models on the entire loading range in each loading mode, the percentage relative error, δ, was obtained according to Eq. (15) and plotted against the strains.

$$\delta = \left(\frac{|\sigma_{\exp} - \sigma_{\text{pred}}|}{\sigma_{\exp}} \right) \times 100 \tag{15}$$

where $\sigma_{\exp}$ and σ_{pred} are the experimental and the predicted stresses respectively. Furthermore, the average value of δ in each loading mode was obtained and, in addition to R^2, used as an indication of the models' accuracy. It should be noted that a perfectly accurate model will have δ that is equal to zero. Finally, the overall behavior of the models in each experimental data was quantified by calculating the overall δ (obtained by summing the average values in each loading mode and dividing by three). We also present the influence of the order number N, in our proposed model's W expression given in Eq. (6) to its accuracy in each loading mode of each experimental data.

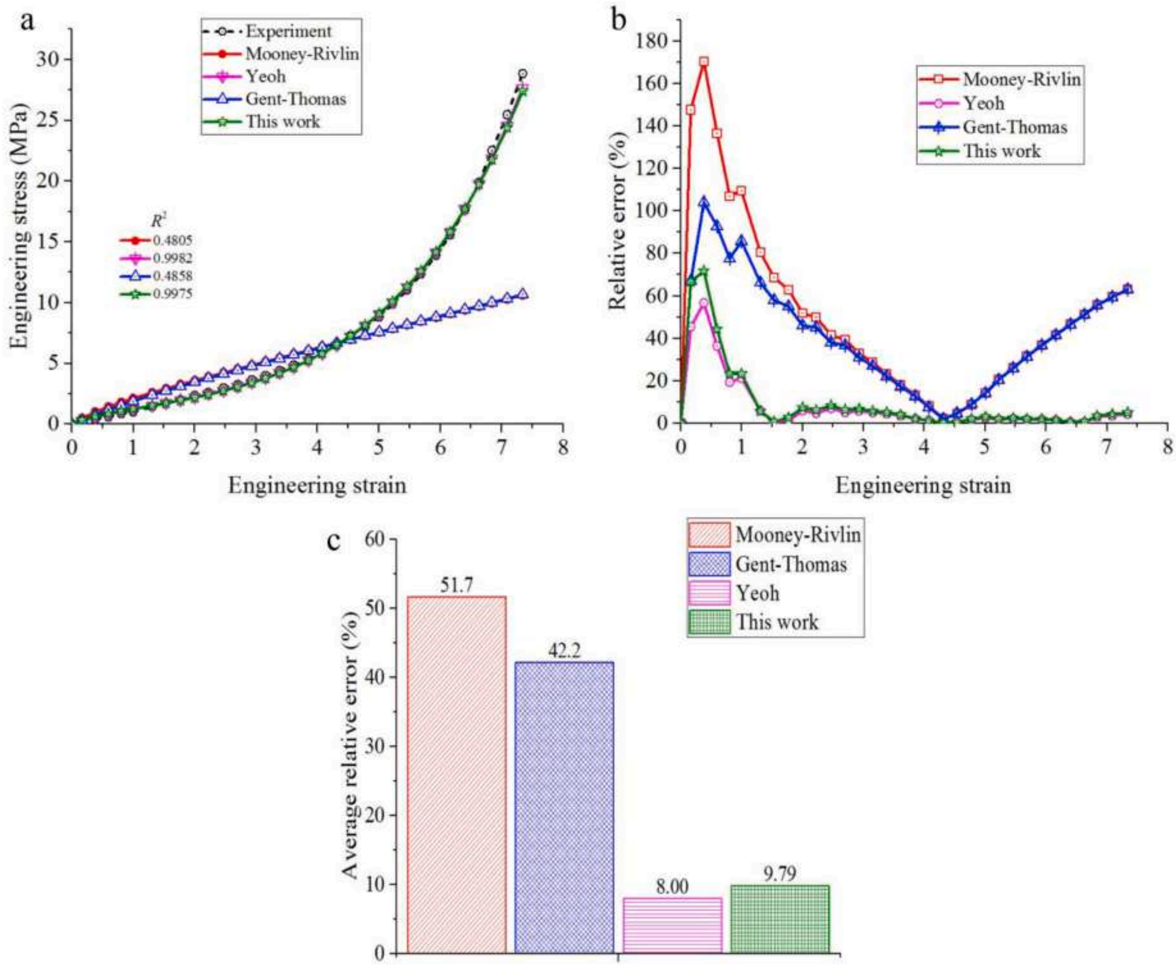

Fig. 7. Comparisons of model performances in reproducing the uniaxial tension experimental data of neoprene rubber by Alexander (Alexander, 1968). (a) stress-strain curves, (b) relative error-strain curves, and (c) the average relative errors.

4.1. Isoprene rubber (Kawabata et al. (Kawabata et al. (1981))

With engineering strains less than 300% in the uniaxial tension loading, it is categorized as moderate deformation. As shown in Fig. 1 (a), the models posted excellent predictions with R^2 values greater than 0.97. The Mooney-Rivlin and the Gent-Thomas models have comparable predictive capabilities as demonstrated in the relative error-strain plots given in Fig. 1 (b) and the average relative errors shown in Fig. 1 (c) whereas our proposed model outperforms all the models with R^2 value greater than 0.99 and average relative error of roughly 1%.

This work's model performed relatively well in describing the equibiaxial loading behavior with R^2 value of 0.95 in contrast to 0.79, 0.87, and 0.83 for Yeoh, Mooney-Rivlin, and Gent-Thomas models respectively as shown in Fig. 2 (a). The relative error-strain plots given in Fig. 2 (b) present a better visualization of the models' performance across the strain range. It is shown that this work's model predictions had the lowest relative errors with an average of 6.77% which was approximately half that of the other models as shown in Fig. 2 (c).

As in the uniaxial tension loading, all the models in this study performed well in pure shear loading with R^2 values of more than 0.93 as shown in Fig. 3 (a). The plot of relative errors against strain given in Fig. 3 (b) shows that this work's model predictions had relatively lower errors with an average of 7.68% compared to over 11% for the other models as shown in Fig. 3 (c). Mostly, relative errors below 10% are acceptable.

4.2. Vulcanized rubber data (Treloar (Treloar (1944))

In the uniaxial tension loading, the vulcanized rubber was subjected to deformations of approximately 650% engineering strain. Thus, it is a case of large deformation and the data has been used extensively in determining the predictive capabilities of new models. At deformation above 450% engineering strain, the Mooney-Rivlin and the Gent-Thomas models stress-strain curves exhibit a linear behavior whereas the experimental curve takes an upturn forming the characteristic S-shaped curve for elastomeric materials at large deformations a shown in Fig. 4 (a) thus leading to severe errors with R^2 values of about 0.57. In contrast, this work's and the Yeoh models capture the upturn behavior accurately with R^2 values greater than 0.99. The relative error-strain plot in Fig. 4 (b) illustrates the behavior of the models throughout the deformation whereby the Mooney-Rivlin and Gent-Thomas models record increasing errors at strain above 450% with about 55% relative errors at maximum strain. As shown in Fig. 4 (c), Yeoh and this work's models posted average relative errors that are less than 5% as opposed to over 20% for Mooney-Rivlin and Gent-Thomas models.

According to the literature, Treloar's equibiaxial loading data is challenging to reproduce as most models post erroneous results. This work's model recorded excellent predictions with R^2 value of above 0.98 in contrast to −0.58, 0.76, and 0.87 for Mooney-Rivlin, Gent-Thomas, and Yeoh models (see Fig. 5 (a)). As mentioned, the negative value of R^2 for Mooney-Rivlin model simply means that the average of the predicted data is far much worse than the average of the experimental data. As shown in Fig. 5 (b), this work's model predictions had the lowest relative

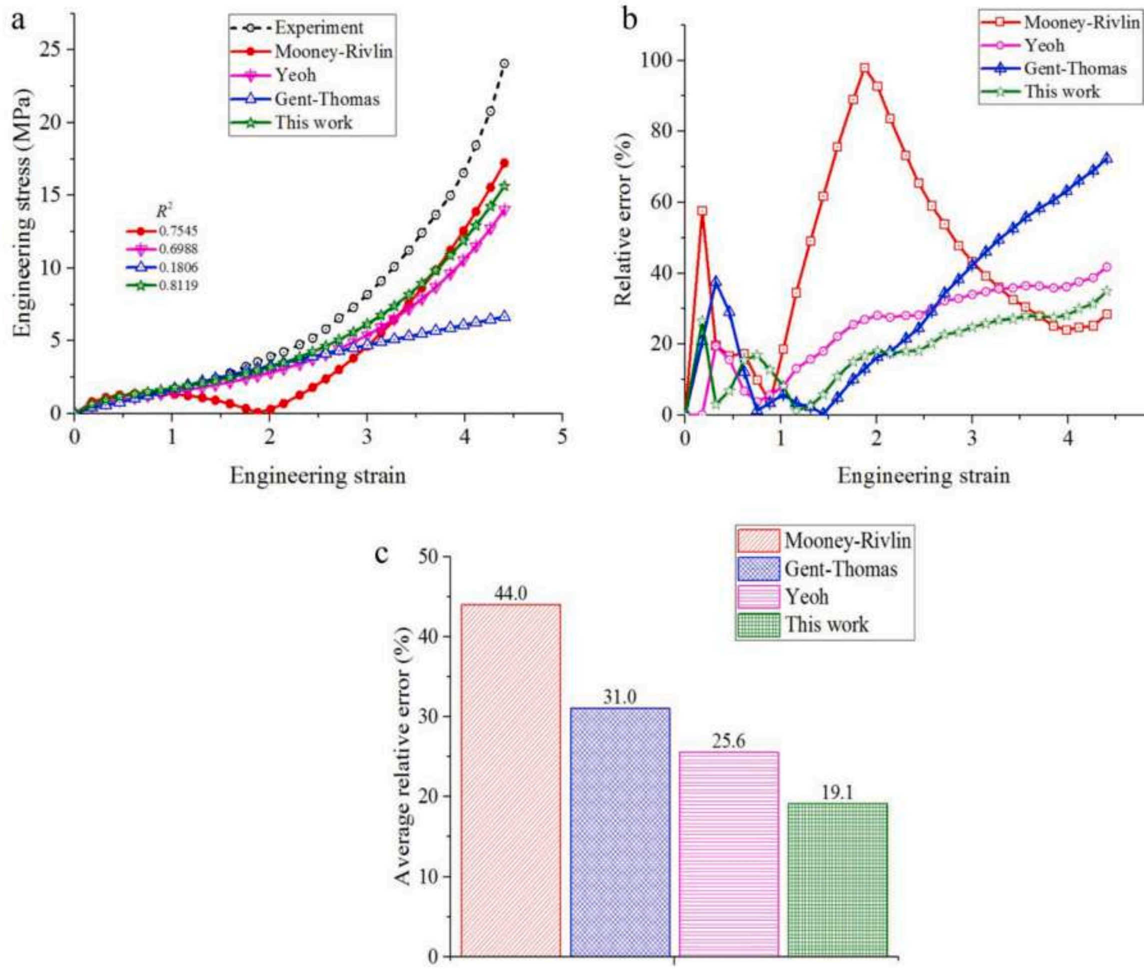

Fig. 8. Comparisons of model performances in reproducing the equibiaxial tension experimental data of neoprene rubber by Alexander (Alexander, 1968). (a) stress-strain curves, (b) relative error-strain curves, and (c) the average relative errors.

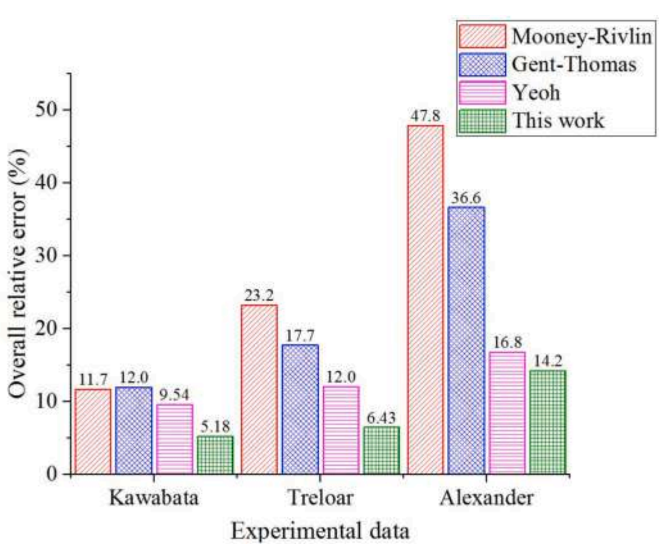

Fig. 9. The overall performance of the models in reproducing the experimental data.

errors with an average of 7.77% as shown in Fig. 5 (c). This is about a third of Yeoh and Gent-Thomas models and about a fifth that of Mooney-Rivlin. Simply put, our proposed model is about three and five times more accurate than Yeoh and Mooney-Rivlin models respectively in the equibiaxial loading data of Treloar.

The stress-strain curves presented in Fig. 6 (a) show that all the models in this study described the pure shear loading satisfactorily with the lowest being the Yeoh model with R^2 value of 0.96. Further analysis of the relative errors in Fig. 6 (b) shows that the models recorded large relative errors of about 20% at engineering strains up to 150%. The average relative errors presented in Fig. 6 (c) demonstrate that the Mooney-Rivlin, Gent-Thomas, and this work's models post acceptable errors of less than 8% whereas the Yeoh model has 11.1%.

4.3. Neoprene rubber data (Alexander (Alexander (1968)))

Neoprene rubber films were subjected to uniaxial and equibiaxial tension loading to about 735% and 440% engineering strains respectively. This data is particularly interesting because it is to a larger deformation relative to the classical Treloar's data and the stress-strain curve has a steep upturn. Expectedly, the Mooney-Rivlin and the Gent-Thomas models posted erroneous predictions with R^2 values of 0.48 as shown in Fig. 7 (a). This is because the models with a linear dependence on the first and the second invariants cannot describe the upturn of the stress-strain curve at large deformations. On the other hand, this work's and Yeoh models captured the behavior accurately with R^2 values of 0.99 as shown in Fig. 7 (a) and minimal relative errors (less than 5%) particularly at large deformations as shown in Fig. 7 (b). The average of the relative error plots in Fig. 7 (c) shows the comparable behavior of this work's and Yeoh models where both have errors below 10%.

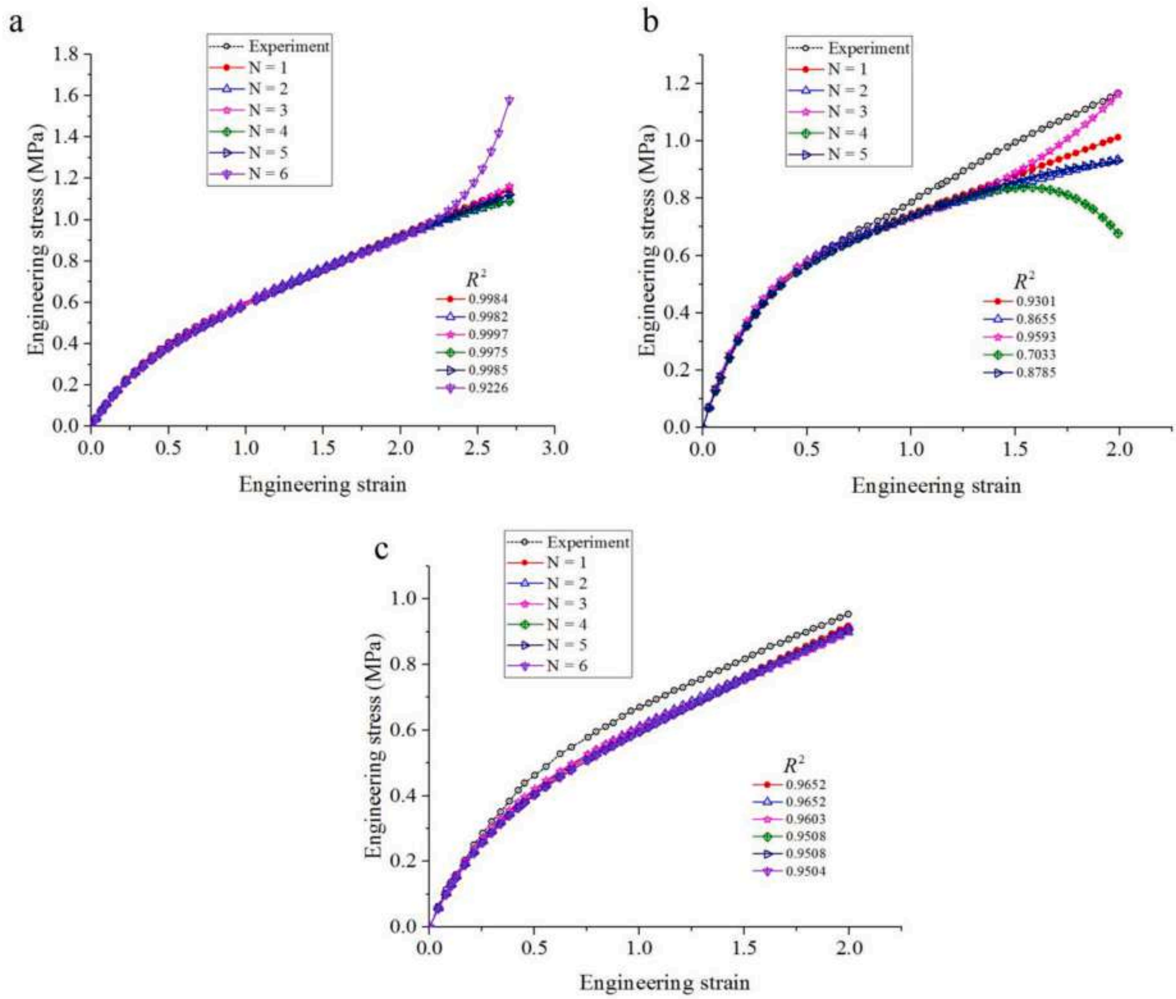

Fig. 10. Comparison of experimental and model-predicted stress-strain curves at different N values for data by Kawabata et al. (Kawabata et al., 1981). (a) uniaxial tension, (b) equibiaxial extension, and (c) pure shear.

The model performances in reproducing the equibiaxial loading data are shown in Fig. 8. It is demonstrated that this work's model predictions are to a relatively higher accuracy based on the R^2 value and the relative errors. It is also demonstrated that the R^2 value alone is not a sufficient indicator of a model's accuracy. The Mooney-Rivlin model posted R^2 value of 0.75 yet had the highest average relative error of 44%.

4.4. *Overall predictive capabilities*

The results from the previous sub-sections demonstrate the fact that hyperelastic models describe experimental behavior in different loading modes to varying accuracy levels. For instance, the errors in the predicted uniaxial tension data may be minimal but significant in equibiaxial tension data. Considering that elastomeric components are subjected to complex loads, evaluating the overall performance of the models is necessary for reliable predictions. To this end, the averages of the average relative errors in each loading mode for each experimental data were utilized to indicate the overall predictive capabilities of the models. As shown in Fig. 9, this work's model recorded relatively lower overall relative errors in all the experimental data. It is also noted that the models performed better in moderate deformations (Kawabata's data) and more errors were recorded in Alexander's data due to the difficulty in reproducing its equibiaxial data.

4.5. *Influence of N*

As this work's model W expression given in Eq. (6) is of polynomial type, it is important to determine the influence of N on the model's accuracy to obtain the optimum number of material parameters. A large number of model parameters renders the model expression overly complicated and leads to non-unique optimal parameter sets. It also complicates the fitting process making it difficult to determine the best set of material parameters that can give accurate and robust predictions in multi-axial loading. There should be a balance between the complexity of the model and the accuracy of the predictions. Too few parameters lead to models that cannot capture the upturn of the stress-strain curve at large deformations. Therefore, values of N ranging from $1-6$ were selected and the model's Cauchy stress expression and predictions were obtained at all the loading modes in each experimental data. It was found that moderate deformations as in the experimental data by Kawabata et al. (1981), N influences both the uniaxial and equibiaxial behavior as shown in Fig. 10 (a) and (b). From $N=1$ to $N=5$, the influence in the uniaxial tension loading was negligible as the predictions posted R^2 values greater than 0.99 and an optimum at $N=3$ of 0.9997. However, at $N=6$ the curves deviate drastically leading to a reduction in R^2 value. For equibiaxial loading in moderate deformations as shown in Fig. 10 (b), it was found that increasing N values lead to unusual behavior in the stress-strain curves with varying levels of accuracy instead of increasing accuracy. This may be attributed to unstable material parameters obtained in the fitting process. The optimum value

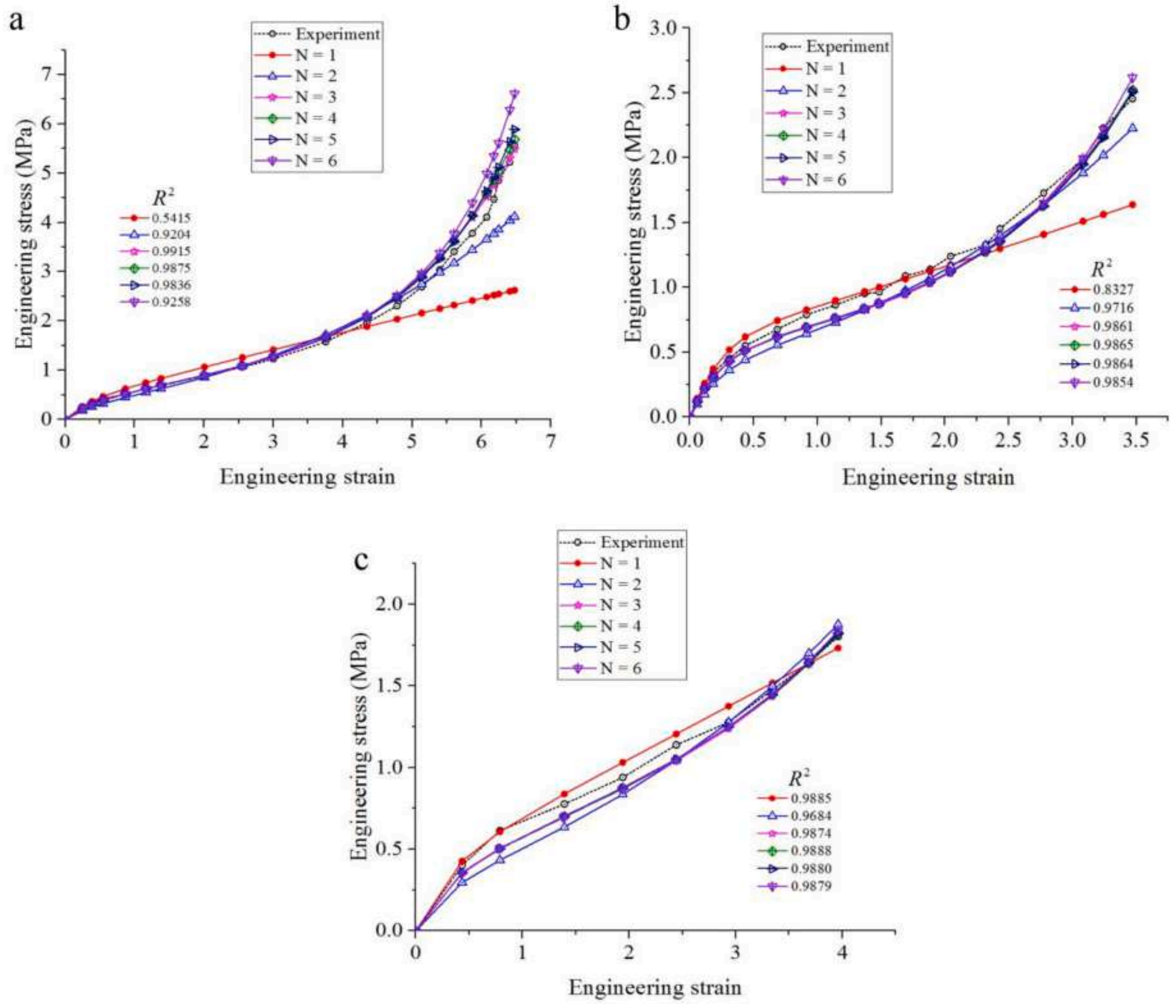

Fig. 11. Model-predicted stress-strain curves at different N values compared to data by Treloar (Treloar, 1944). (a) uniaxial tension, (b) equibiaxial extension, and (c) pure shear.

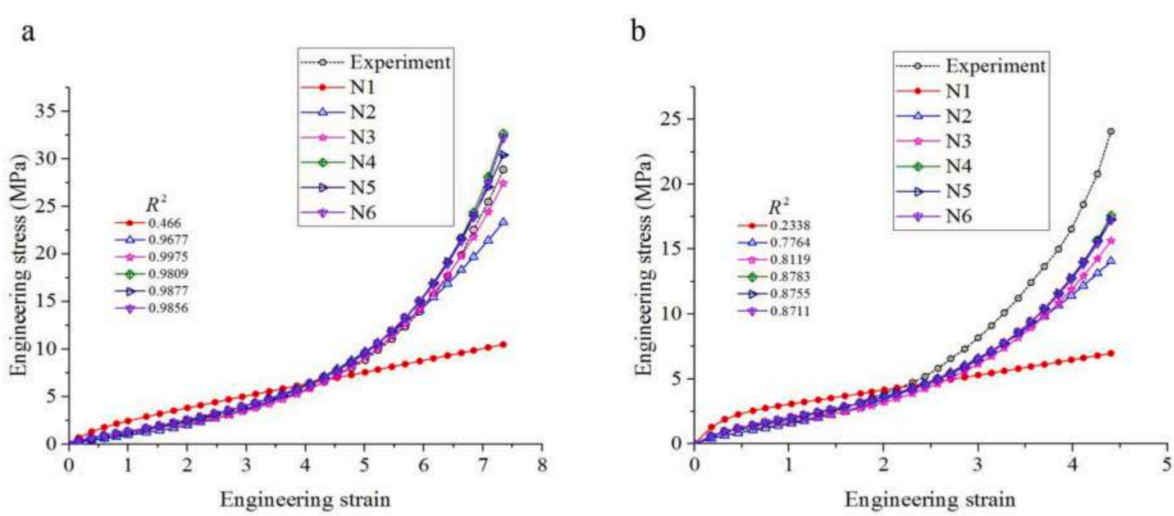

Fig. 12. Model-predicted stress-strain curves at different N values compared to data by Alexander (Alexander, 1968). (a) uniaxial tension and (b) equibiaxial tension.

for equibiaxial loading is found to be 0.9593 at $N = 3$ whereas the curve at $N = 6$ deviated so much that decided against including it. From Fig. 10 (c), it is shown that N has a negligible effect on pure shear loading predictions. As demonstrated in Fig. 10, only a single term of our proposed model, i.e. $N = 1$, suffices is reproducing the experimental data for moderate deformations in all the loading modes to high accuracy levels.

For large deformation as in the data by Treloar (1944) and Alexander

(1968), N was found to significantly impact the accuracy of the predicted data in the uniaxial tension loading. As shown in Fig. 11 (a), the accuracy in the uniaxial tension increases with N value up to an optimum R^2 of 0.9915 at $N = 3$ and thereafter a drop in accuracy with increasing N. Similarly, increasing N yielded better predictions in equibiaxial tension up to $N = 3$ where further increase had a negligible effect on the accuracy as shown in Fig. 11 (b). Only at $N = 2$ were the predictions in the pure shear loading of relatively lower accuracy with R^2 of 0.96 as shown in Fig. 11 (c) whereas the rest stood at 0.98. The difference is insignificant and, therefore, we can conclude that it does not affect the pure shear loading of Treloar's data. Owing to the large deformation and steep upturn of the neoprene rubber stress-strain curves, N has a significant effect on the accuracy of the model predictions in both uniaxial and equibiaxial loadings as demonstrated in Fig. 12. The optimum N value for uniaxial tension is found to be 3 whereas, in equibiaxial tension, the accuracy is improved up to $N = 4$ where a further increase in N value becomes insignificant to the R^2 value.

5. Conclusions

Phenomenological constitutive models of hyperelastic materials are more popular than their micromechanical counterparts thanks to their relative advantages such as the ease of obtaining material parameters and applicability to a wide range of materials. Important features of a phenomenological model concern its capability to describe experimental behavior in three loading modes (uniaxial tension, equibiaxial extension, and pure shear), the process of calibrating the model equation to obtain its parameters, and the number of experimental data sets required. As the practical loading on an elastomeric component involves complex three-dimensional loads, it is imperative that the model accurately describes the experimental behavior in the three loading modes from moderate to large deformations for reliable designs. Furthermore, the model parameters should be obtained in a single fitting process using easily available experimental data such as the uniaxial tension other than obtaining each parameter individually or requiring data from multiple loading modes as it increases the complexity, time, and the cost of the fitting process.

With inspiration from the generalized Rivlin model, this work proposed a polynomial-type phenomenological model whose strain energy density function expression has linear and logarithmic first and second invariants of the Cauchy-Green deformation tensor respectively. Its predictive capabilities in the entire deformation range of hyperelastic materials were determined by utilizing three sets of experimental data from the literature. The coefficient of determination, commonly known as R-squared, is the most common quantity that is utilized to indicate how the predicted data correlates with the experimental data. However, it is not sufficient to rely on only the R-squared especially when the predictive performances of several models are to be compared as comparable values do not necessarily mean comparable predictive behavior. Therefore, obtaining the relative errors at every strain point and their averages for every loading mode is necessary for the complete characterization of models' predictive abilities. Based on R-squared values, relative error-strain plots, and average relative errors, this work's model was found to better describe the experimental response in comparison to three popular models from the literature. Models with a linear dependence on the invariants of the Cauchy-Green deformation tensor fail to describe the characteristic S-shaped stress-strain curve at large deformations. The order of a polynomial model significantly affects the accuracy of the predicted data particularly in the uniaxial and equibiaxial loading at large deformation. There is an optimum order beyond which further increase is insignificant to the model's accuracy and may lead to severe errors in the predictions. Consequently, it is crucial to determine the optimum order for a polynomial model. It was found to have a negligible effect on the pure shear loading and the optimum value (wherein the uniaxial and equibiaxial predictions for both moderate and large deformation were to a relatively higher accuracy) was established to be 3. With the ability to describe the moderate and large deformation response of various elastomeric materials whilst requiring fitting by only the uniaxial extension data as demonstrated in this work, the proposed model is suitable for application in the design of elastomeric components.

Credit author statement

Stephen Kirwa Melly: Conceptualization, Methodology, Software, Formal analysis, Data curation, Writing – original draft. **Liwu Liu**: Conceptualization, Methodology, Validation, Writing – review & editing. **Yanju Liu**: Conceptualization, Methodology, Validation, Writing – review & editing. **Jinsong Leng**: Writing – review & editing, Resources, Supervision, Funding acquisition.

Declaration of competing interest

The authors declare that they have no known competing financial interests or personal relationships that could have appeared to influence the work reported in this paper.

Acknowledgments

This work was supported by the National Natural Science Foundation of China (Grant Nos. 11632005, 12072094, and 12172106).

References

Alexander, H., 1968. A constitutive relation for rubber-like materials. Int. J. Eng. Sci. 6 (9), 549–563.
Anssari-Benam, Afshin, Bucchi, Andrea, 2021. A generalised neo-Hookean strain energy function for application to the finite deformation of elastomers. Int. J. Non Lin. Mech. 128, 103626.
Anssari-Benam, Afshin, Bucchi, Andrea, Saccomandi, Giuseppe, 2021. On the central role of the invariant I2 in nonlinear elasticity. Int. J. Eng. Sci. 163, 103486.
Arruda, Ellen M., Boyce, Mary C., 1993. A three-dimensional constitutive model for the large stretch behavior of rubber elastic materials. J. Mech. Phys. Solid. 4 (2), 389–412.
Bahreman, Marzieh, Darijani, Hossein, Fooladi, Majid, 2016. Constitutive modeling of isotropic hyperelastic materials using proposed phenomenological models in terms of strain invariants. Polym. Eng. Sci. 56 (3), 299–308.
Bergström, Jörgen, 2015. Mechanics of Solid Polymers: Theory and Computational Modeling. William Andrew.
Bale Baidi Blaise, Liman Kaoye Madahan Bien-aimé, Betchewe, Gambo, Marckman, Gilles, Beda, Tibi, 2020. A phenomenological expression of strain energy in large elastic deformations of isotropic materials. Iran. Polym. J. (Engl. Ed.) 29, 525–533.
Biderman, V.L., 1958. Calculation of rubber parts (in Russian). Rascheti na prochnost 40.
Bischoff, Jeffrey E., Arruda, Ellen M., Grosh, Karl, 2001. A new constitutive model for the compressibility of elastomers at finite deformations. Rubber Chem. Technol. 74 (4), 541–559.
Carroll, M.M., 2011. A strain energy function for vulcanized rubbers. J. Elasticity 103, 173–187.
Dal, Hüsnü, Açikgöz, Kemal, Badienia, Yashar, April 2021. On the Performance of Isotropic Hyperelastic Constitutive Models for Rubber-like Materials: A State of the Art Review. Applied Mechanics Reviews. https://doi.org/10.1115/1.4050978 [Online].
Destrade, Michel, Giuseppe Saccomandi, Sgura, Ivonne, 2017. Methodical fitting for mathematical models of rubber-like materials. Proc. R. Soc. A. 473 (2198), 20160811.
Doll, S., Schweizerhof, K., 2000. On the development of volumetric strain energy functions. J. Appl. Mech. 67 (1), 17–21.
Francisco Lalo, Debora, Greco, Marcelo, Meroniuc, Matias, 2019. Numerical modeling and experimental characterization of elastomeric pads bonded in a conical spring under multiaxial loads and pre-compression. Mathematical Problems in Engineering, p. 5182629. https://doi.org/10.1155/2019/5182629.
Gent, A.N., Thomas, A.G., 1958. Forms for the stored (strain) energy function for vulcanized rubber. J. Polym. Sci. 28 (118), 625–628.
Gornet, Laurent, Desmorat, R., Marckmann, Gilles, Charrier, Pierre, 2012. A new isotropic hyperelastic strain energy function in terms of invariants and its derivation into a pseudo-elastic model for Mullins effect: application to finite element analysis. In: Stephen, Jerrams, Murphy, Niall (Eds.), Constitutive Models for Rubber VII. CRC Press, pp. 265–271.
Horgan, C.O., Murphy, J.G., 2007. Constitutive models for almost incompressible isotropic elastic rubber-like materials. J. Elasticity 87, 133–146.

Horgan, Cornelius O., Murphy, Jeremiah G., 2009. On the volumetric part of strain-energy functions used in the constitutive modeling of slightly compressible solid rubbers. Int. J. Solid Struct. 46, 3078–3085.

Kaliske, M., Heinrich, G., 1999. An extended tube-model for rubber elasticity: statistical-mechanical theory and finite element implementation. Rubber Chem. Technol. 72 (4), 602–632.

Kawabata, S., Matsuda, M., Tei, K., Kawai, H., 1981. Experimental survey of the strain energy density function of isoprene rubber vulcanizate. Macromolecules 14 (1), 154–162.

Khajehsaeid, H., Arghavani, J., Naghdabadi, R., 2013. A hyperelastic constitutive model for rubber-like materials. Eur. J. Mech. Solid. 38, 144–151.

Levenberg, Kenneth, 1944. A method for the solution of certain non-linear problems in least squares. Q. Appl. Math. 2 (2), 164–168.

Melly, Stephen Kirwa, Liu, Liwu, Liu, Yanju, Leng, Jinsong, 2021. Improved Carroll's hyperelastic model considering compressibility and its finite element implementation. Acta Mech. Sin. https://doi.org/10.1007/s10409-021-01064-4.

Marquardt, Donald W., 1963. An algorithm for least-squares estimation of nonlinear parameters. J. Soc. Ind. Appl. Math. 11 (2), 431–441.

Mooney, M., 1940. A theory of large elastic deformation. J. Appl. Phys. 11 (9), 582–592.

Muhr, A.H., 2005. Modeling the stress-strain behavior of rubber. Rubber Chem. Technol. 78 (3), 391–425.

Murphy, J.G., Rogerson, G.A., 2018. Modelling slight compressibility for hyperelastic anisotropic materials. J. Elasticity 131, 171–181.

Paul, Steinmann, Hossain, Mokarram, Possart, Gunnar, 2012. Hyperelastic models for rubber-like materials: consistent tangent operators and suitability for Treloar's data. Arch. Appl. Mech. 82, 1183–1217.

Ogden, Raymond William, 1972. Large deformation isotropic elasticity — on the correlation of theory and experiment for incompressible rubberlike solids. Proc. R. Soc. Lond. A 326 (1567), 565–584.

Rivlin, R.S., 1948. Large elastic deformations of isotropic materials. IV. Further developments of the general theory. Phil. Trans. Roy. Soc. Lond. 241, 379–397.

Rivlin, R.S., Saunders, D.W., 1951. Large elastic deformations of isotropic materials VII. Experiments on the deformation of rubber. Phil. Trans. Roy. Soc. Lond. Math. Phys. Sci. 243 (865), 251–288.

Treloar, L.R.G., 1944. Stress-strain data for vulcanized rubber under various types of deformation. Rubber Chem. Technol. 17 (4), 813–825.

Treloar, L.R.G., 1975. The Physics of Rubber Elasticity, third ed. Oxford University Press, USA.

Upadhyay, Kshitiz, Subhash, Ghatu, Douglas, Spearot, 2019. Thermodynamics-based stability criteria for constitutive equations of isotropic hyperelastic solids. J. Mech. Phys. Solid. 124, 115–142.

Upadhyay, Kshitiz, Subhash, Ghatu, Douglas, Spearot, 2020a. Hyperelastic constitutive modeling of hydrogels based on primary deformation modes and validation under 3D stress states. Int. J. Eng. Sci. 103314, 154.

Upadhyay, Kshitiz, Subhash, Ghatu, Douglas, Spearot, 2020b. Visco-hyperelastic constitutive modeling of strain rate sensitive soft materials. J. Mech. Phys. Solid. 135, 103777.

Xiang, Yuhai, et al., 2018. A general constitutive model of soft elastomers. J. Mech. Phys. Solid. 117, 110–122.

Yeoh, O.H., 1993. Some forms of the strain energy function for rubber. Rubber Chem. Technol. 66 (5), 754–771.